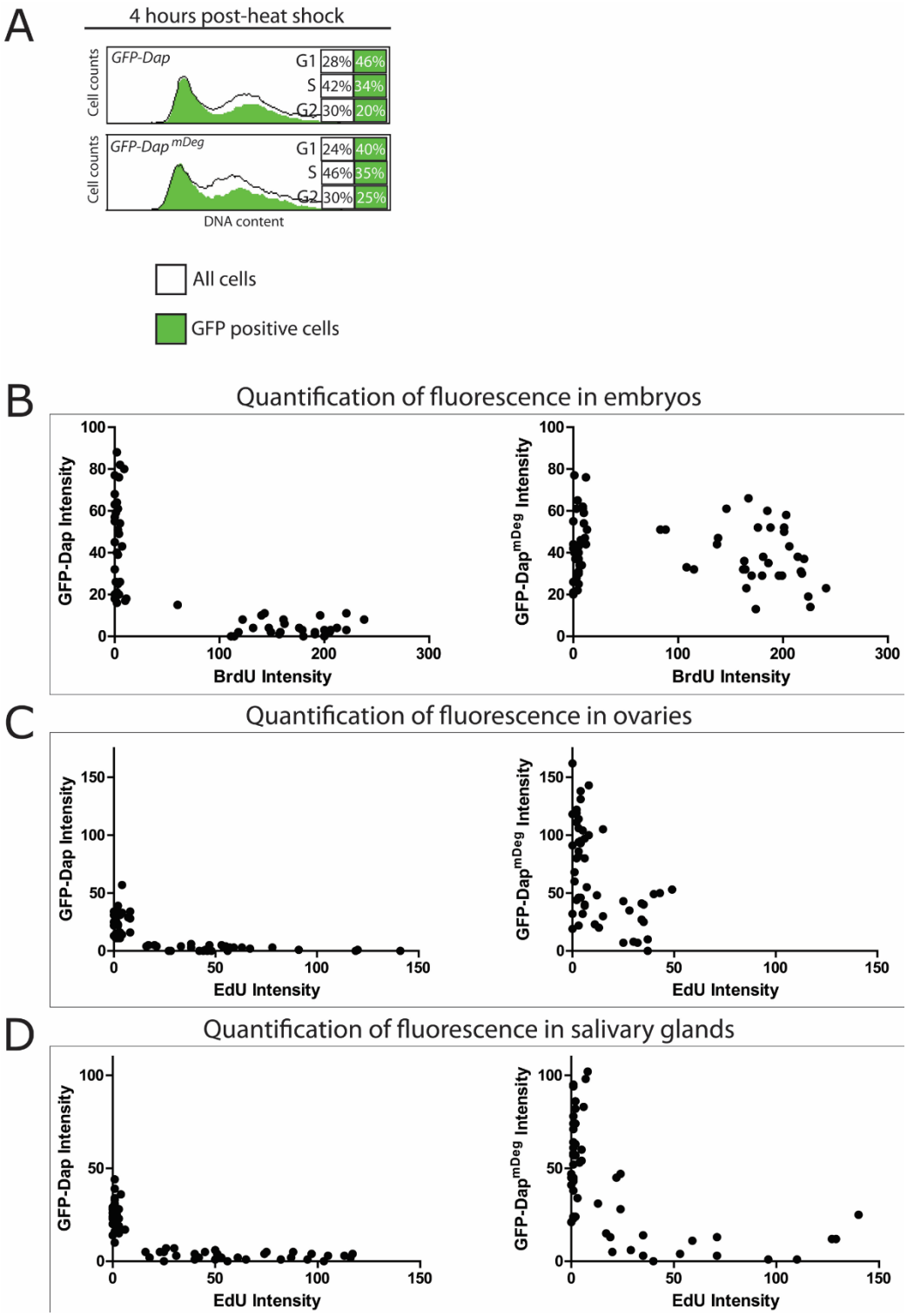

Fig. S1. Mutation of the PIP degron does not inhibit Dap function in S2 cells. (A) Flow cytometric analysis of GFP-Dap^{mDeg} 4 hours following heat shock. At this time point there is an increase in the percentage of GFP-positive cells in G1 compared to the total cell

population, as expected since Dap inhibits Cyclin E/Cdk2 and therefore S-phase entry. (B) Alternate representation of the data shown in Figure 1H. Quantification of fluorescence in 5 hour old *tub>GFP-Dap* (left) and *tub>GFP-Dap*^{mDeg} (right) embryos. Each point represents a single cell; three embryos per genotype were used for quantification. (C) Alternate representation of the data shown in Figure 4F. Quantification of fluorescence in Stage 10 *c323>GFP-Dap* (left) and *c323>GFP-Dap*^{mDeg} (right) ovarian follicle cells. Each point represents a single cell; three egg chambers per genotype were used for quantification. (D) Alternate representation of the data shown in Figure 5H. Quantification of fluorescence in *ptc>GFP-Dap* (left) and *ptc>GFP-Dap*^{mDeg} (right) salivary glands. Each point represents a single cell; three glands per genotype were used for quantification.

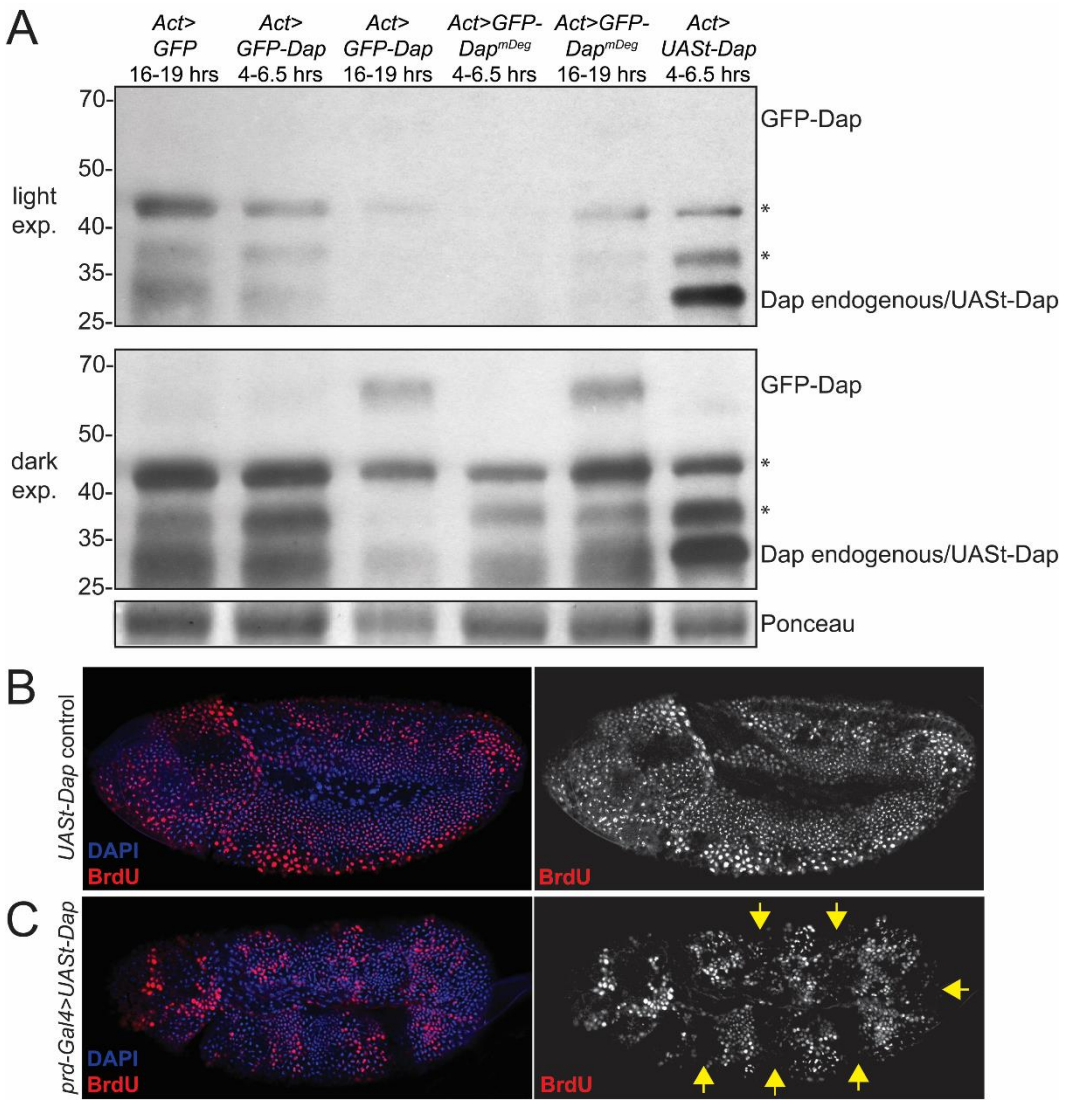

Fig. S2. UASp-Dap transgenes activate lower levels of expression than UASt-Dap. (A) Embryos were collected from *act-Gal4/CyO* mothers crossed to homozygous UAS-GFP or UAS-Dap lines. Therefore, ~50% of the embryos express the indicated transgene. Hours indicate age of embryos after egg deposition. UASt-Dap is from Lane et al (1996), and all other UAS-Dap transgenes are from this study. Both blots were probed with anti-Dap antibodies and stained with Ponceau to indicate loading, which was approximately 30 embryos per lane. Two exposures are shown. While Dap expressed from UASt is visible at 4-6.5 hrs AED at levels much higher than endogenous Dap, transgenic GFP-Dap cannot be

detected. We could detect GFP-Dap expression at a later embryonic time point (16-19 hrs); i.e. after a longer period of expression. Non-specific bands are indicated with *, and protein size markers (in kDa) are indicated to the left. (B-C) Five hour old *UASt-Dap* control (B) and *prd-Gal4>UASt-Dap* (C) embryos labeled with BrdU (red) and DAPI (blue). Note the suppression of BrdU incorporation in *prd-GAL4*-expressing stripes (yellow arrows).

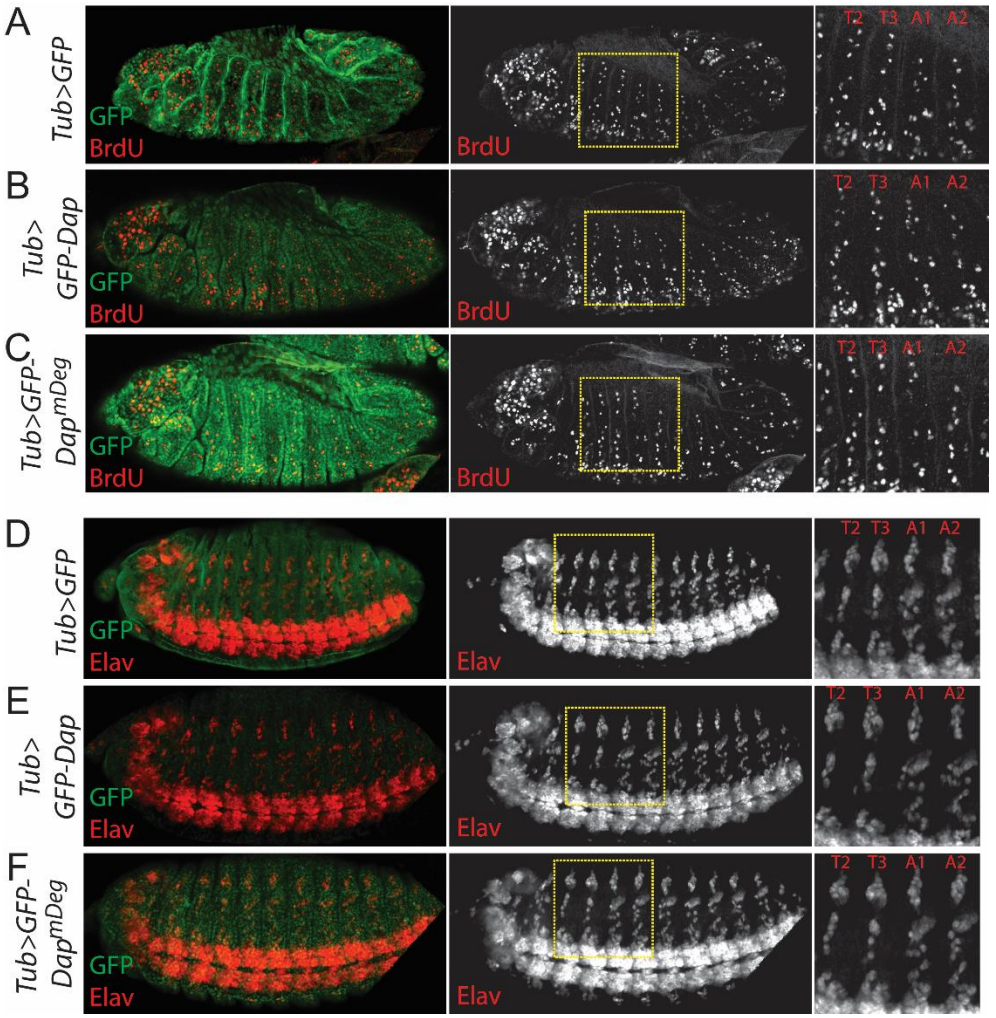

Fig. S3. S phase-stabilized Dap does not overtly alter nervous system development. (A-C) Stage 12 embryos expressing GFP or the indicated GFP-Dap transgenes with *tub-GAL4* and labeled with BrdU (red) and anti-GFP antibodies (green). We were unable to detect significant differences in BrdU incorporation throughout the central or peripheral nervous systems in *tub>GFP*, *tub>GFP-Dap*, or *tub>GFP-Dap*^{mDeg} embryos. (D-F) Stage 13 embryos expressing GFP or the indicated GFP-Dap transgenes with *tub-GAL4* and labeled with and anti-GFP antibodies (green) and anti-ELAV antibodies (red) to examine neuronal differentiation. We were unable to detect significant differences in the pattern of ELAV staining among *tub>GFP*, *tub>GFP-Dap*, or *tub>GFP-Dap*^{mDeg} embryos. Yellow boxes outline areas shown at higher magnification in panels on right; T2 and T3 = thoracic segments 2 and 3; A1 and A2 = abdominal segments 1 and 2.

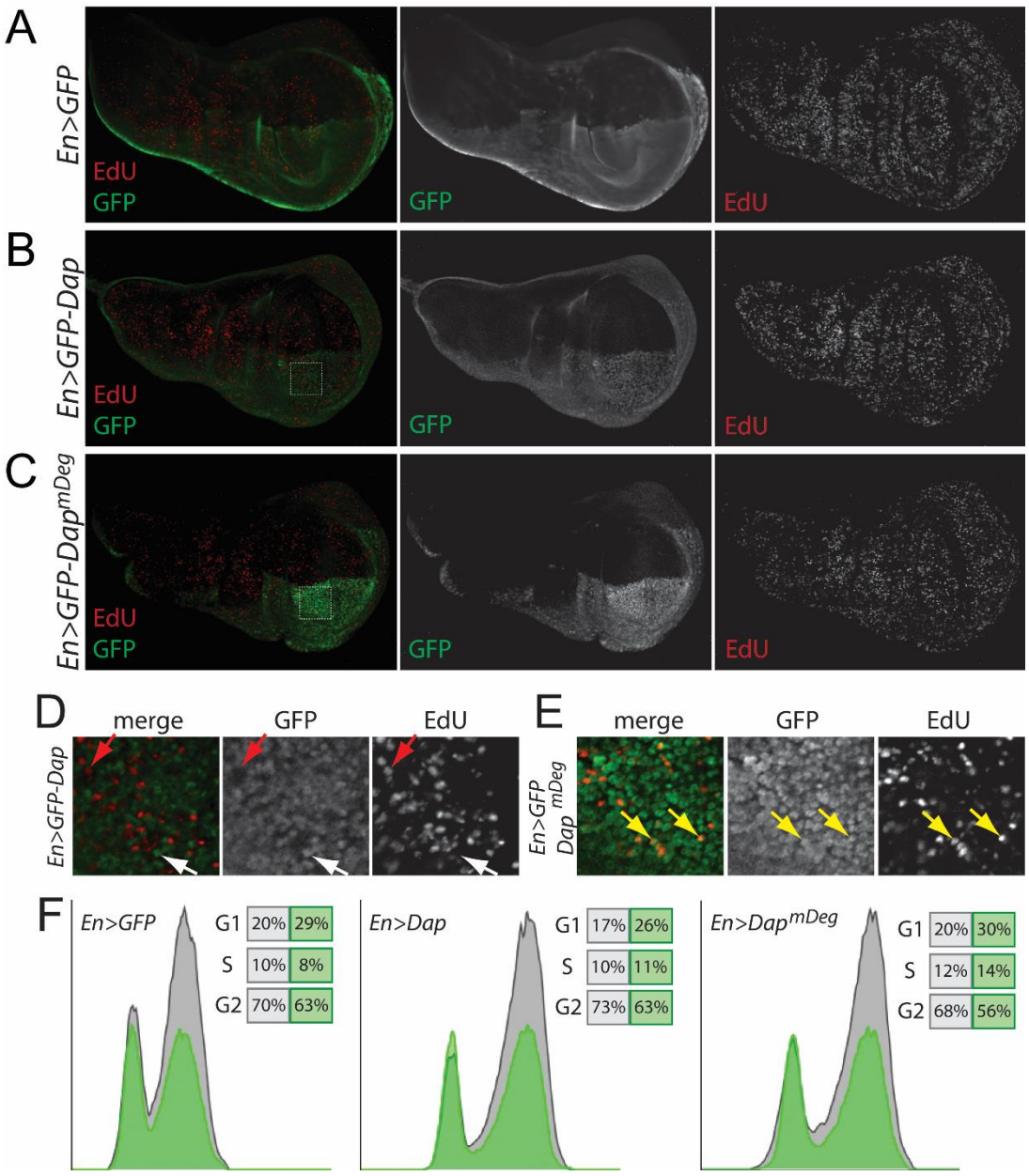

Fig. S4. Normal proliferation in the wing imaginal disc in the presence of S phase-stabilized Dap. (A-C) Third larval instar wing imaginal discs expressing GFP, GFP-Dap, or GFP-Dap^{mDeg} in the posterior compartment with *en-GAL4* and labeled with EdU (red) and anti-GFP antibodies (green). We noted no obvious differences in S phase in the anterior versus posterior compartment in any of the three genotypes. (D, E) High magnification images of the region indicated with the white boxes in panels B and C. GFP-Dap accumulates in EdU-negative nuclei (white arrows) but not in EdU positive nuclei (red arrows). In

contrast, GFP-Dap^{mDeg} accumulates in most nuclei, including those labeled with EdU (yellow arrows). (F) Wing discs expressing GFP alone or in combination with GFP-Dap or GFP-Dap^{mDeg} under the control of *en-GAL4* were dissociated and DNA content were analyzed by flow cytometry. The grey histogram represents GFP- cells (anterior compartment, no transgene expressed) and the green histogram represents GFP+ cells (posterior compartment, transgenes expressed). The histograms shown are from one representative experiment, while the % cell cycle phase is an average from two (GFP) or three (GFP-Dap and GFP-Dap^{mDeg}) experiments.

Table S1. Parameter values for the updated endocycle model.

Parameter	Value	Source
Le2f	2.01737×10^{-2}	Zielke et al.
HE2F	4.95696×10^{1}	Zielke et al.
Lrbf	1.28355×10^{-1}	Zielke et al.
HRBF	4.76255×10^{1}	Zielke et al.
Ccyce	6.38521×10^{-2}	Zielke et al.
Lcyce	6.41289×10^{-2}	Zielke et al.
Cbase	1.41396×10^{-2}	Zielke et al.
Hcyce	1.56612×10^{1}	Zielke et al.
HCYCE	1.55936×10^{1}	Zielke et al.
Ldup	8.96353×10^{-2}	Zielke et al.
HDUP	7.29125×10^{1}	Zielke et al.
Lgem	2.74846×10^{-1}	Zielke et al.
HGEM	1.22268×10^{2}	Zielke et al.
HCUL	1.04044×10^{1}	Zielke et al.
KRE	1.03072×10^{-2}	Zielke et al.
KER	7.61116×10^{-2}	Zielke et al.
KERp	7.47067×10^{-1}	Zielke et al.
KND	1.20893×10^{-1}	Zielke et al.
KGD	2.67595	Zielke et al.
KDG	2.6062×10^{-1}	Zielke et al.
kCULe	6.83866×10^{-2}	Zielke et al.
nuCULe	5	Zielke et al.
CULmaxE	2.87638×10^{-1}	Zielke et al.
kCr	1.14596×10^{-2}	Zielke et al.
nuCr	5	Zielke et al.
PmaxR	5.02815×10^{-2}	Zielke et al.
DmaxR	7.43329×10^{-2}	Zielke et al.
kEc	4.08772×10^{-1}	Zielke et al.
nuEc	7	Zielke et al.
kRc	8.74772×10^{-2}	Zielke et al.
nuRc	1	Zielke et al.
Dcyce	1.54073×10^{1}	Zielke et al.
DRC	4.05764×10^{1}	Zielke et al.
maxA	1.62473×10^{-2}	Zielke et al.

CmaxA	6.46459×10^{2}	Zielke et al.
kCa	7.39395×10^{-1}	Zielke et al.
nuCa	4	Zielke et al.
AmaxG	2.23532×10^{-1}	Zielke et al.
kAg	2.78149×10^{-1}	Zielke et al.
nuAg	7	Zielke et al.
CULmaxD	7.23261×10^{-1}	Zielke et al.
kCULd	1.13506×10^{-1}	Zielke et al.
nuCULd	1	Zielke et al.
kRCc	1.05168×10^{-1}	Zielke et al.
nuRCc	7	Zielke et al.
RCmaxC	8.00826×10^{-2}	Zielke et al.
kCp	6.54308×10^{-2}	Zielke et al.
nuCp	3	Zielke et al.
CmaxP	6.25876×10^{-2}	Zielke et al.
kCYCED	1.5×10^{-3}	This Study
Ldap	9.5×10^{1}	This Study
HDAP	1.15×10^{-1}	This Study
CYCEmaxD	1.05×10^{-1}	This Study
nuCD	1	This Study
CULmaxDAP	6.5×10^{-1}	This Study
kCULD	$5.\times10^{-2}$	This Study
DAPmaxC	9.5×10^{-1}	This Study
kDAPC	4.5×10^{-1}	This Study
nuDC	3	This Study